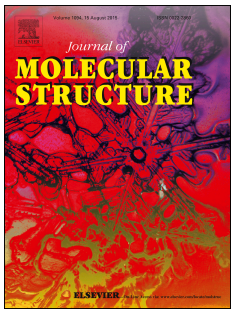

Silver(I) and gold(I) complexes with sulfasalazine: Spectroscopic characterization, theoretical studies and antiproliferative activities over Gram-positive and Gram-negative bacterial strains

Ana Thereza Fiori-Duarte, Raphael Enoque F. de Paiva, Carlos M. Manzano, Wilton R. Lustri, Pedro P. Corbi

PII: S0022-2860(20)30483-X

DOI: https://doi.org/10.1016/j.molstruc.2020.128158

Reference: MOLSTR 128158

To appear in: *Journal of Molecular Structure*

Received Date: 24 January 2020

Revised Date: 23 March 2020

Accepted Date: 29 March 2020

Please cite this article as: A.T. Fiori-Duarte, R.E.F. de Paiva, C.M. Manzano, W.R. Lustri, P.P. Corbi, Silver(I) and gold(I) complexes with sulfasalazine: Spectroscopic characterization, theoretical studies and antiproliferative activities over Gram-positive and Gram-negative bacterial strains, *Journal of Molecular Structure* (2020), doi: https://doi.org/10.1016/j.molstruc.2020.128158.

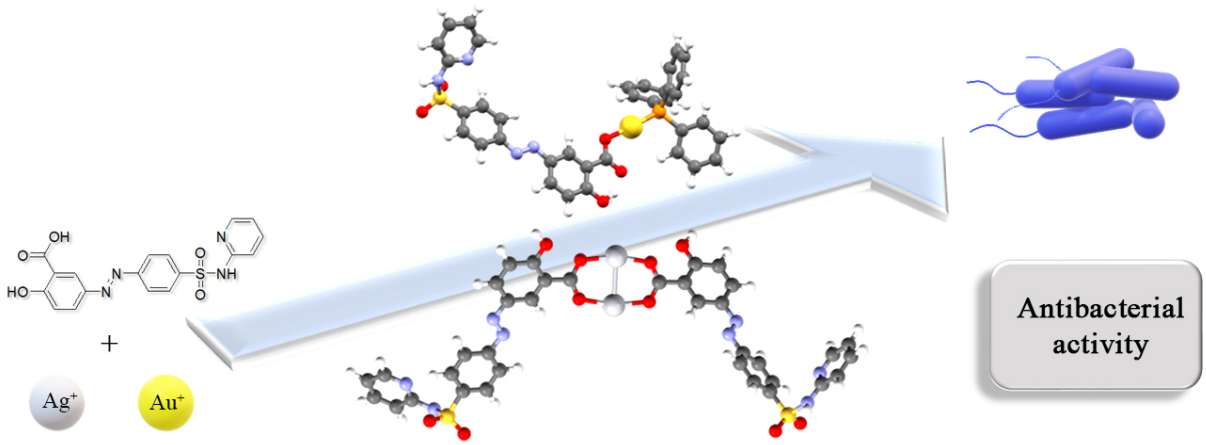

Silver(I) and gold(I) complexes with sulfasalazine: spectroscopic characterization, theoretical studies and antiproliferative activities over Gram-positive and Gram-negative bacterial strains

Ana Thereza Fiori-Duarte[1,2], Raphael Enoque F. de Paiva[3], Carlos M. Manzano[1], Wilton R. Lustri[4], Pedro P. Corbi[1*]

[1] *Institute of Chemistry, University of Campinas – UNICAMP, P.O. Box 6154, 13083-970 Campinas, SP, Brazil.*

[2] *Faculty of Pharmaceutical Sciences, University of Campinas – UNICAMP, 13083-871 Campinas, SP, Brazil.*

[3] *Institute of Chemistry, University of São Paulo – USP, 05508-000 São Paulo, SP, Brazil.*

[4] *Biological and Health Sciences Department – University of Araraquara-UNIARA, 14801-320 Araraquara, SP, Brazil.*

* Corresponding author: ppcorbi@unicamp.br

ABSTRACT

The emergence of bacterial strains resistant to antibiotics, such as the sulfonamides (sulfa drugs), is currently a case of concern. The synthesis of metal complexes using well-known antibacterial agents and bioactive metals has proven to be an excellent strategy in the development of new and more active metallodrugs. Herein, we report the synthesis, structural characterization and antibacterial analysis of new gold(I) and silver(I) complexes with the sulfa drug sulfasalazine (ssz). Elemental, thermal and high-resolution mass spectrometric measurements indicated a 1:1:1 Au/ssz/Ph_3P molar composition for the gold(I) complex (Ph_3P - triphenylphosphine), while for the silver(I) complex the molar composition was 1:1 Ag/ssz. Solution state NMR and infrared spectroscopic data suggest that ssz coordinates to silver(I) and gold(I) by the oxygen atoms of the deprotonated carboxylic group. The coordination mode of the carboxylate was supported by density functional theory (DFT) calculations, which reinforces a monodentate coordination for the gold(I) complex and a bridged bidentate mode for the silver(I) one, with the molecular formulas [(Ph_3P)Au(ssz)] and $[Ag(ssz)]_2$, respectively. Antibacterial activity assays indicated the sensitivity of Gram-positive (*Staphylococcus aureus* and *Bacillus cereus*) and Gram-negative (*Escherichia coli* and *Pseudomonas aeruginosa*) bacterial strains to $[Ag(ssz)]_2$ and [(Ph_3P)Au(ssz)] complexes, while the free ligand was not able to inhibit the growth of any tested bacteria. The non-interaction of the complexes with deoxyribonucleic acid (DNA) was also demonstrated, which suggests that this biomolecule is not a preferential target for the compounds.

KEYWORDS

Sulfasalazine; Silver(I); Gold(I); Mass spectrometry; DFT; Antibacterial activity.

Abbreviation list (in alphabetical order)

$[Ag(ssz)]_2$ – silver(I) complex with sulfasalazine;

ATCC - American Type Culture Collection;

BHI - Brain Heart Infusion;

CFU - Colony Forming Unit;

CisPt – Cisplatin;

DFT - Density Functional Theory;

DMSO - Dimethylsulfoxide;

DNA - Deoxyribonucleic acid;

ESI-QTOF-MS - Electrospray Ionization Quadrupole Time-of-Flight Mass Spectrometry;

IR - Infrared vibrational spectroscopy;

MIC - Minimum Inhibitory Concentration;

NMR - Nuclear Magnetic Resonance;

(Ph_3P) – Triphenylphosphine;

[(Ph_3P)AuCl] - Chloro(triphenylphosphine)gold(I);

[(Ph_3P)Au(ssz)] - Gold(I) complex with sulfasalazine;

ssz – Sulfasalazine;

SYBR Green - Nucleic acid gel electrophoresis stain;

TG/DTA - Thermogravimetric and Differential Thermal Analyses;

1. Introduction

The emergence of bacterial resistance to antibiotics is currently considered as a case of concern by the World Health Organization (WHO). The lack of effective antibiotics could have catastrophic effects on well-established modern medical procedures, such as organ transplantation and general surgeries, cancer therapy and chronic disease treatments [1,2]. The excessive use of the current antibiotics and the lack of development of new drugs is among the main causes related to the crisis of bacterial resistance [3].

In this context, one of the strategies for the development of new active compounds for the treatment of infectious diseases is the combination of the already known antibacterial drugs, such as the sulfonamides (sulfa drugs) with bioactive metals, such as silver and gold, among others [4], seeking an improvement of activity by a synergistic or additive effect [5–7]. In the viewpoint of coordination chemistry, the use of sulfa drugs is an excellent strategy because they are endowed with coordinating atoms and, in some cases, the metal complexes have shown to be more effective than the free sulfas over bacterial strains [8–11].

The sulfonamides were the first chemotherapeutic agents used to treat bacterial infections [12,13]. Sulfasalazine (ssz, 2-hydroxy-5-[[4-(pyridin-2-ylsulfamoyl)phenyl]diazenyl]benzoic acid, $C_{18}H_{14}N_4O_5S$**, Figure 1**), is a sulfonamide derived from mesalazine and it has shown to possess antibacterial and anti-inflammatory activities, being classified as a nonsteroidal anti-inflammatory drug of the salicylate class. It is used to treat chronic diseases such as rheumatoid arthritis and inflammatory bowel diseases (e.g., ulcerative colitis and Crohn's disease) [14–18]. According to the pH medium, sulfasalazine can exist in four forms in solution: neutral (non-ionized) and three ionized forms associated with deprotonation of carboxyl group (pKa_1 = 2.35), sulfonamide and hydroxyl groups [19].

In addition to the antimicrobial activity, there are descriptions of sulfonamide-derived drugs and its complexes that have shown to be effective *in vitro* and *in vivo* for the treatment of various types of cancer [8,20–22]. Recently, the use of sulfasalazine to improve the treatment of radio-resistant cancers was demonstrated in a study by Nagane et al., where sulfasalazine decreased intratumoral glutathione content, increasing radiosensitivity in an *in vivo* transplanted melanoma model [23].

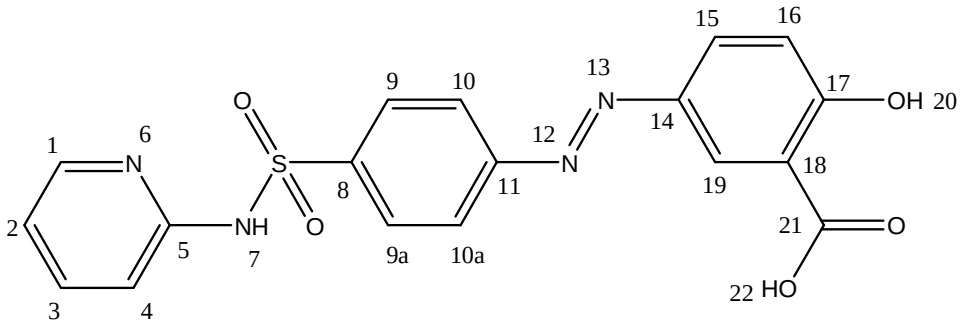

Fig. 1. Structure of sulfasalazine with carbon, hydrogen and nitrogen atoms numbered.

Refat et al. synthesized and characterized sulfasalazine complexes and evaluated their biological activities. The manganese(II), mercury(II), chromium(III) and yttrium(III) complexes were prepared and evaluated for their antimicrobial and antifungal activities by an antibiogram assay. In this study, the mercury(II) complex was shown to be active against *Tricoderma* sp., with an inhibition zone of 20 mm of diameter while sulfasalazine did not show inhibition in the same experimental conditions [14]. There are also descriptions in the literature from the same group on the synthesis of magnesium(II), calcium(II), strontium(II) and barium(II) complexes with sulfasalazine. The strontium(II) complex showed higher activity than the free ligand and the other complexes against *Staphylococcus aureus* (*S. aureus*), *Escherichia coli* (*E. coli*), *Bacillus anthracis* (*B. anthracis*), *Pseudomonas aeruginosa* (*P. aeruginosa*) and the fungi *Candida albicans* (*C. albicans*) [24]. A copper(II) complex with sulfasalazine and triphenylphosphine as ligands, with coordination formula $[Cu(C_{18})H_{13}N_4O_5S)(Ph_3P)_2]$, where Ph_3P is triphenylphosphine, was also described in the literature, but no biological studies were performed [25].

Gold(I) complexes with sulfonamides have also shown to be promising as antimicrobial agents. Mizdal et al. presented the synthesis of five gold complexes with sulfadiazine and sulfamethoxazole. Minimum inhibitory concentration (MIC) assays against MRSA (methicillin-resistant S. *aureus*) and strains of the same species obtained from clinical isolates showed the better activity of all five complexes in comparison to the free ligands. The MIC of the gold(I) complexes with sulfamethoxazole against MRSA were all between 2 and 8 µg/mL, while the MIC of sulfamethoxazole alone was 256 µg/mL [26].

Silver complexes with sulfonamides have also been extensively investigated as antibacterial agents. In special, silver sulfadiazine (AgSSD) can be considered as the most successful example of the use of sulfa in coordination chemistry. This complex is used clinically worldwide in the treatment of bacterial skin infections in burn wounds [27]. Since the discovery of the action of AgSSD, many other silver complexes have been investigated for the treatment of bacterial infections. Some examples include the silver(I) complexes with sulfamoxole (SMX), $[Ag_2(SMX)_2]\cdot H_2O$ and $[Ag_4(SCN)_3(SMX)]\cdot H_2O$, which exhibit antimicrobial activity against *E. coli, S. aureus* and *P. aeruginosa* strains, and also antifungal action (against ten fungi strains) [28].

In the last years, our research group has dedicated efforts in the search of novel and bioactive metal complexes with sulfonamides. Paiva et al. demonstrated the antibacterial activity of a silver(I) complex with the anti-inflammatory nimesulide over Gram-positive and Gram-negative bacteria [29]. Nunes et al. synthesized silver(I) complexes with the sulfonamides sulfathiazole and sulfamethoxazole and evaluated their antibacterial activity. The MIC values over *S. aureus*, *P. aeruginosa* and *Salmonella enterica* ranged from 3.45 to 6.90 mmol L^{-1} for the sulfathiazole complex and 1.74 to 13.9 mmol/L for the sulfamethoxazole one [30].

Similarly, silver(I) complexes with sulfisoxazole, sulfadimethoxine [31] and sulfameter [32] were synthesized and exhibited antibacterial activities against *S. aureus*, *P. aeruginosa* and *E. coli* with MIC values in the micromolar range. In all these examples, the free sulfonamides were not able to inhibit any of the bacteria strains in the considered experimental conditions. Yamamoto et al. reported copper(II) and silver(I) complexes with sulfamethizole that were active over the same bacteria strains in the low milimolar range, between 3.31 and 0.41 mmol L^{-1} [33].

More recently, Nakahata et al. studied the biological properties of three new copper(II) complexes with the sulfonamides sulfameter and sulfadimethoxine, where the nuclease activity of the complexes were correlated with their anti-*M. tuberculosis* profiles and also with their antitumoral activities (total growth inhibition in the micromolar range) over a variety of cancer cell lines, specially glioma (U251), melanoma (UACC-62), ovarian (OVCAR-3) and colon (HT29) [34].

In this work, we present the synthesis of new gold(I) and silver(I) complexes with sulfasalazine and its characterization combining theoretical and experimental data. The antibacterial activities of the complexes and the biophysical studies about the interaction of the compounds with DNA are also described here for the first time.

2. Materials and methods

2.1.Materials

Sulfasalazine (ssz ≥ 98%) and silver(I) nitrate ($AgNO_3$ ≥ 99%) were purchased from Sigma-Aldrich/Merck Laboratories. Tetrachloroauric(III) acid trihydrate (≥ 49% Au) was obtained from Acros Organics. Sodium hydroxide (≥ 97%), triphenylphosphine (≥ 98%) and triethylamine (N(CH□CH□)□ ≥ 99%) were obtained from Vetec. SYBR Green and cisplatin were also purchased from Sigma-Aldrich/Merck Laboratories. Deoxyribonucleic acid (DNA) Ladder 1Kb Plus (1200 bp) was purchased from Invitrogen. All chemical reagents were used as received.

2.2.Equipment

Elemental analyses for carbon, hydrogen and nitrogen were performed using a Perkin Elmer 2400 CHNS/O Analyzer. Thermogravimetric and differential thermal analyses (TG/DTA) were performed on a simultaneous TGA/DTA SEIKO EXSTAR 6000 thermal analyzer, using the following conditions: synthetic air, flow rate of 50 cm^3 min^{-1} and heating rate of 10°C min^{-1}, from 25°C to 900°C. X-Ray powder diffraction analyses were performed on a Shimadzu XRD 7000 diffractometer. Infrared (IR) spectroscopic analyses were performed in an Agilent Cary 630 FTIR spectrometer, using the Attenuated Total Reflectance (ATR) method, in the range from 4000-400 cm^{-1} and with resolution of 4 cm^{-1}. Solution state ^1H and ^{13}C nuclear magnetic resonance (NMR) spectra were recorded in Bruker Avance III 400 MHz, 500 MHz and 600 MHz spectrometers. The NMR spectra were acquired in DMSO-d6. The chemical shifts were given relative to tetramethylsilane (TMS). Electrospray ionization quadrupole time-of-flight mass spectrometric (ESI-QTOF-MS) measurements were performed on a XEVO-QTOF-MS instrument operating in the positive mode. The samples were dissolved in 10 μL of DMSO and then diluted in a 1:1 H_2O/CH_3CN solution containing 0.1% of formic acid (v/v). The instrumental parameters of the acquisition were: capillary voltage 3.5 kV, sampling cone voltage 30 V, source temperature 150°C, desolvation temperature 150 °C and collision energy 6 eV. Electrophoresis system BIO-RAD® (Sub-Cell® GT) was used for the agarose gel electrophoresis studies.

2.3.Synthesis of the silver complex

The silver complex was synthesized by the reaction of 5.0 x 10^{-4} mol (0.0844 g) of a freshly prepared 1:1 methanol/water solution of $AgNO_3$ (10.0 mL) with a solution containing 5.0 x 10^{-4} mol (0.1993 g) of sulfasalazine in 20.0 mL of a 1:1 methanol/water solution. The pH of the final solution was adjusted to 8-9 by the addition of NaOH 0.10 mol/L solution. The synthesis was carried out under stirring and at room temperature for 2 hours. A brownish solid was obtained and vacuum filtered, washed with cold water and dried in a desiccator over P_4O_{10}. Elemental analysis led to a 1:1 Ag/ssz composition. Anal. Calcd. for $AgC_{18}H_{13}N_4O_5S$ (%): C, 42.8; H, 2.59; N, 11.1. Found (%): C, 43.0; H, 2.59; N, 11.1. The silver complex is soluble in DMSO. No single crystals were obtained considering crystal growth techniques such as mixture of solvents or recrystallization for a detailed X-ray crystallographic study.

2.4.Synthesis of the gold(I) complex

First, the chloro(triphenylphosphine)gold(I) precursor ([$(Ph_3P)AuCl$]) was prepared by the reaction of 5.0 x 10^{-4} mol (0.1967 g) of tetrachloroauric(III) acid trihydrate ($HAuCl_4 \cdot 3H_2O$) dissolved in 1.0 mL of a 1:1 ethanol/acetone solution, with 1.0 x 10^{-3} mol (0.2626 g) of triphenylphosphine (Ph_3P) dissolved in 1.0 mL of chloroform. The synthesis was carried out under stirring at room temperature and after a few minutes a white solid was obtained, filtered off and washed with ethanol.

Subsequently, a freshly prepared solution of [$(Ph_3P)AuCl$] (1.25 x 10^{-4} mol, 0.0616 g) in 3.0 mL of chloroform was added to a solution of sulfasalazine (1.25 x 10^{-4} mol, 0.0498 g) and triethylamine (0.25 mL) in methanol (4 mL). The synthesis was carried out under reflux for 24 hours. After slow evaporation an orange solid was obtained. Elemental analysis led to a 1:1:1 Au/ssz/Ph_3P composition, plus one triethylamine molecule. Anal. Calcd. for $AuPC_{36}H_{28}N_4O_5S \cdot N(CH\square CH\square)\square$ (%): C, 52.7; H, 4.53; N, 7.31. Found (%): C, 51.8; H, 4.74; N, 7.45. The [$(Ph_3P)Au(ssz)$] complex is soluble in dimethylsulfoxide (DMSO) and chloroform and low soluble in water, ethanol, methanol, acetonitrile and acetone. Again, no single crystals were obtained for a detailed X-ray crystallographic study.

2.5.DFT studies

The structures of the silver(I) and gold(I) complexes were optimized using the Density Functional Theory (DFT) as implemented in Orca 4.2 [35,36]. For the gold compound, the hybrid functional PBE0, along with the triple-zeta def2-TZVP basis set were used. Auxiliary Weigend basis were used [37]. Due to the size of the system, for the silver compound the def2-SVP basis set was used. A grid size of 5 and a tight SCF convergence criteria were used for both systems. The final figures were rendered with JMol 14.29.53.

2.6.Antibacterial activity assays

The antibacterial activities of the precursors and the silver(I) and gold(I) complexes were determined over four referenced bacterial strains, *S. aureus* ATCC 25923, *Bacillus cereus* (*B. cereus*) ATCC 14579, *E. coli* ATCC 25922 and *P. aeruginosa* ATCC 27853 using the minimum inhibitory concentration (MIC) method. The microorganisms were cultured in separate test tubes containing 10.0 mL of sterile brain heart infusion (BHI) and incubated for 18h at 35-37 °C, following the recommendations of the Clinical and Laboratory Standards Institute [38]. An inoculum from each culture was added to new tubes with sterile BHI until the turbidity measured was 1.0 McFarland ($\sim 3.0 \cdot 10^8$ CFU·mL^{-1}; CFU = Colony Forming Units). Stock solutions of the sulfonamide and complexes were prepared in DMSO 10% (10.0 mg·mL^{-1}). The tested compounds were sequentially diluted with BHI medium in 96 multi-well plate for a final volume of 100 µL/well. An inoculum of 100 µL of the bacterial strains in BHI suspension at 1.0 McFarland scale was added to each serial dilution reaching turbidimetric 0.5 McFarland ($\sim 1.5 \cdot 10^8$ CFU·mL^{-1}) in a final volume of 200 µL/well at concentrations ranging from 2000 µg·mL^{-1} to 31.25 µg·mL^{-1}. The plate was incubated for 18h at 35-37 °C in a damp chamber under stirring at 100 rpm. The first well of the microplate was used as a negative control, containing 60 µL of sterile BHI, 40 µL of the DMSO 10% and 100 µL of the bacterial suspension on the 1.0 McFarland scale. As a positive control, a solution of silver nitrate was used. After the incubation period, 15 µL of resazurin 0.02% in sterile aqueous solution was added to each well. After 3h of re-incubation the MIC were estimated as reported in the literature [38].

2.7.Agarose gel electrophoresis

The experimental procedure for the agarose gel electrophoresis assay was similar to previous reports in the literature [39–41]. In this assay, samples of ssz, silver(I) and gold(I) complexes were first solubilized in DMSO; $AgNO_3$ and K_2PdCl_4 were solubilized in water and cisplatin (CisPt) was suspended in water. Then, all samples were diluted in phosphate buffer (HPO_4^{2-}/ $H_2PO_4^-$, pH = 7.4) to 250 $\mu mol \cdot L^{-1}$. Aliquots (6 or 3 µL) of each compound were mixed with pGEX-4T1 plasmid DNA solution (19 µL) to final concentrations of 60 $\mu mol \cdot L^{-1}$ or 30 $\mu mol \cdot L^{-1}$ of the compounds in phosphate buffer. After the incubation (37 °C, 18 hours), the loading buffer (bromophenol blue 0.25 % m/v, xylene cyanol 0.25 % m/v, glycerol 30% m/v and EDTA 30 $mmol \cdot L^{-1}$ in sterile distilled water; 5 µL per sample) was added to each sample. The samples were applied to a 0.8% agarose gel matrix in Tris-Borate-EDTA 0.5x buffer at pH 8.3 and electrophoresed for 2 hours at 100 V. The pGEX-4T1 plasmid was used as control and DNA Ladder 1Kb Plus (1200 bp) was used as a weight marker. The gel was stained with 1 x SYBR green for 3 h and photodocumented using a UVDoc 400i Delpho equipment. The pGEX-4T1 plasmid DNA was provided by Professor Wilton Rogério Lustri from the Biological and Health Sciences Department/ University of Araraquara-UNIARA, Brazil.

3. Results and discussion

3.1.*Thermal analysis*

The gold(I) and silver(I) complexes and the free sulfasalazine were evaluated by thermogravimetric (TG) and differential thermal analyses (DTA) in order to confirm the proposed molar compositions of the complexes, and to evaluate the thermal stability of the compounds.

The thermal decomposition of sulfasalazine occurs in two steps. The first starts at 238 °C and ends at 322 °C, while the second one starts at 430 ºC and ends at 618 °C. No residue was observed at 900 °C (**Supplementary Material, Fig. S1**). The thermal decomposition of the silver(I) complex also occurs in two exothermic steps. The first one starts at 230 °C and ends at 312 °C and the second starts at 403 °C and ends at 520 °C. The percentage of mass loss in the two steps is consistent with the release of one

ligand ($C_{18}H_{13}N_4O_5S$). Calcd. loss of $C_{18}H_{13}N_4O_5S$: 78.6%. Found: 76.4%. A residue of 23.6% is observed at 770 °C, which is consistent with the formation of metallic silver. Calcd.: 21.3%; Found: 23.6% (**Supplementary Material, Fig. S2**). For the gold(I) complex, the thermal decomposition also occurs in two exothermic steps. The first one starts at 106 °C and ends at 380 °C and the second starts at 444 °C and ends at 676 °C. The percentage of mass loss in the two steps is consistent with one ligand ($C_{18}H_{13}N_4O_5S$), one triphenylphosphine ($PC_{18}H_{15}$) and one triethylamine ($C_6H_{15}N$). Calcd. for organic mass loss of $AuPC_{36}H_{28}O_5N_4S{\cdot}C_6H_{15}N$: 79.4%. Found: 75.9%. A residue of 24.1% is observed at 730 °C, which is consistent with the formation of metallic gold. Calcd. for Au□ residue: 20.6%. Found: 24.1% (**Supplementary Material, Fig. S3**). The identity of the thermal residue obtained from the decomposition of the gold(I) complex was confirmed as metallic gold by powder X-ray diffraction analysis of the residue (**Supplementary Material, Fig. S4**).

3.2.Infrared absorption spectroscopy

To confirm the coordination of the ligand to metal ions and to determine the possible coordination sites, infrared (IR) spectroscopic measurements were performed. The IR spectra (**Supplementary Material, Fig. S5**) obtained for the complexes were analyzed in comparison to the spectrum of the ligand in its anionic form (sodium salt).

The coordination mode of the carboxylate (COO^-) group to the metal can be determined by the separation ($\Delta\nu$) between its asymmetric and symmetric stretching modes. Absorption bands at 1627 and 1424 cm^{-1} ($\Delta\nu$ 203 cm^{-1}) in the IR spectrum of the sodium salt of sulfasalazine were observed and attributed to the asymmetric (ν_{as}) and symmetric stretching (ν_s) of the carboxylate group, respectively. For the silver(I) and gold(I) complexes, bands at 1634 and 1430 cm^{-1} ($\Delta\nu$ 204 cm^{-1}) and at 1631 and 1391 cm^{-1} ($\Delta\nu$ 240 cm^{-1}), respectively, were observed and assigned to the asymmetric (ν_{as}) and symmetric stretching (ν_s) of the carboxylate group.

It is well-established in the literature [42] that when $\Delta\nu$ of the carboxylate group in a metal complex is similar to the $\Delta\nu$ of the ligand, a bridged bidentate mode of the COO^- group is expected, while when the $\Delta\nu$ of the complex is greater than the ligand, a monodentate coordination mode by the carboxylate group is suggested. Therefore, based on the resolution of the equipment (4 cm^{-1}), there are no changes in the $\Delta\nu$ values when the IR spectrum of the ligand is compared to the silver(I) complex, which is an

indication that the carboxylate group coordinates to the silver(I) by a bridged bidentate mode. For the gold(I) complex, the higher Δν value for the carboxylate group when compared to the ligand suggests a monodentate coordination mode. Moreover, no significant changes in the asymmetric and symmetric stretching modes of the sulfone group in the IR spectrum of the ligand when compared to the spectra of the complexes, which indicates that the sulfonamide group does not participate in the coordination of sulfasalazine to the metal atoms.

3.3.NMR spectroscopic measurements

Solution state ^{1}H (**Figure 2**) and ^{13}C NMR spectra (**Supplementary Material, Fig. S6 and S7**) of the silver(I) and gold(I) complexes were obtained in order to identify the coordination sites of sulfasalazine to silver(I) and gold(I). The spectra of the complexes were analyzed by comparison with the NMR spectrum of the sulfasalazine.

By analyzing the ^{1}H and ^{13}C spectra of the silver(I) and gold(I) complexes and comparing it to the spectra of the ligand, it was observed that the major chemical shifts Δδ (δ complex – δ ligand) refer to the hydrogen and carbon atoms present in the salicylic ring of sulfasalazine. The hydrogen atoms H15 and H16 and the carbon atoms C14, C15, C17 and C18 have shown to be the most affected ones upon coordination (**Table 1**). This result reinforces the suggested coordination modes of sulfasalazine to silver(I) and gold(I) by the carboxylate group, which is present in the salicylic ring of sulfasalazine, as suggested by the infrared spectroscopic data [43].

The ^{1}H and ^{13}C spectra also confirms the presence of a molecule of triethylamine in the composition of the gold(I) complex as already stated by other techniques. There were observed peaks at 1.15 and 3.03 ppm in the ^{1}H NMR spectrum and at 9.36 and 46.1 ppm in the ^{13}C spectrum of the gold(I) complex, which refer to triethylamine used in the synthesis to deprotonate the ligand. Such spectra can be seen at the **Supplementary Material, Fig. S8 and S9.**

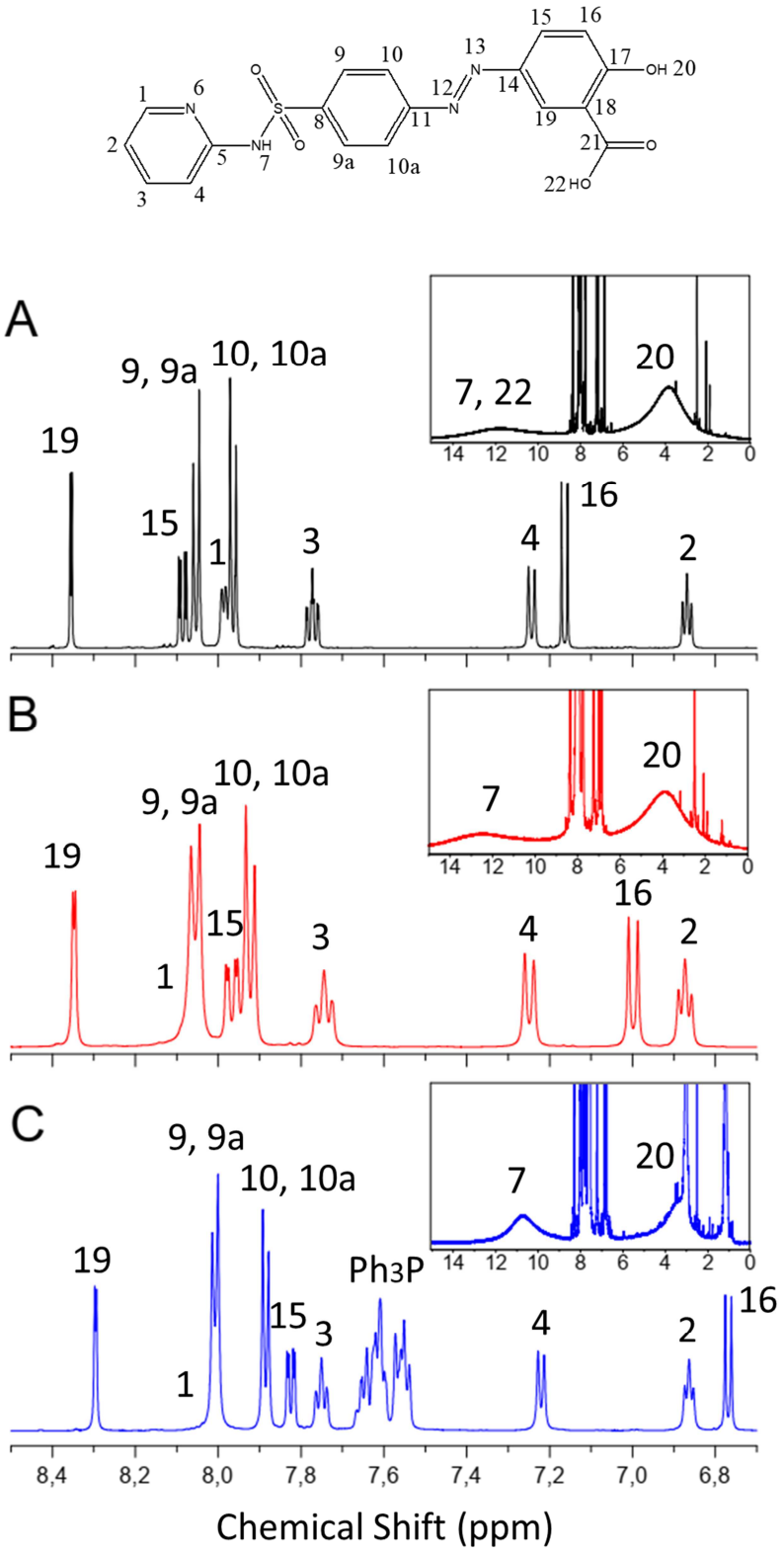

Fig. 2. ^{1}H NMR spectra in DMSO-d_6 of (A) sulfasalazine, (B) silver(I) complex and (C) gold(I). The insets (increased intensities) show the signals corresponding to H7 and H20.

Table 1. ^{1}H and ^{13}C NMR assignments and chemical shifts for sulfasalazine, silver(I) and gold(I) complexes in ppm. For hydrogen and carbon atoms numbering, see **Figure 1**.

Assignment	Sulfasalazine (δ)	Silver(I) complex (δ)	Δδ (ppm)	Gold(I) complex (δ)	Δδ
H1	7.99	8.05	0.06	8.00	0.01
H2	6.87	6.87	0.0	6.86	-0.01
H3	7.77	7.75	-0.02	7.75	-0.02
H4	7.24	7.24	0.0	7.22	-0.02
H7	15.0 – 10.0	14.0 – 11.0		12.0 – 9.0	
H9, H9a	8.06	8.05	-0.01	8.00	-0.06
H10, H10a	7.96	7.92	-0.04	7.88	-0.08
H15	8.09	7.97	-0.12	7.82	-0.27
H16	7.17	6.99	-0.18	6.76	-0.41
H19	8.36	8.34	-0.02	8.29	-0.07
H20	5.00 – 3.00	5.00 – 3.00		5.00 – 2.00	
H22	15.0 – 10.0				
C1	154.14	154.25	0.11	154.12	-0.02
C2	114.96	115.06	0.10	115.45	0.49
C3	141.87	140.81	-1.06	141.34	-0.53
C4	114.39	114.37	-0.02	114.67	0.28
C5	154.14	154.21	0.11	154.12	-0.02
C8	144.44	143.42	-1.02	143.01	-1.43
C9, C9a	128.28	127.90	-0.38	128.21	-0.07
C10, C10a	123.21	122.45	-0.76	122.56	-0.65
C11	153.86	153.66	-0.20	154.56	0.70
C14	114.96	116.53	1.57	119.59	4.63
C15	129.56	128.12	-1.44	127.51	-2.05
C16	119.03	118.21	-0.82	118.64	-0.39
C17	164.69	166.44	1.75	170.91	6.22
C18	144.89	143.64	-1.25	142.71	-2.18
C19	126.87	126.53	-0.34	127.20	0.33
C21	171.72	171.05	-0.67	171.07	-0.65

3.4.Mass spectrometric measurements

The silver(I) and gold(I) complexes were analyzed by ESI(+)-QTOF-MS and the corresponding full spectra are presented in **Figure 3.**

For the silver complex, two monoprotonated ions were identified in the spectrum (**Figure 4**). The first peak corresponds to the $[Ag(C_{18}H_{13}N_4O_5S) + H]^+$ ion at *m/z* 506.98, while the second one is attributed to the $[Ag_2(C_{18}H_{13}N_4O_5S)_2 + H]^+$ ion at *m/z* 1011.03. The peak at *m/z* 399.05 corresponds to the free ionized sulfasalazine $[(C_{18}H_{14}N_4O_5S) + H]^+$. This result confirms the proposed 1:1 metal/ligand composition and that the complex might exist in a dimeric form, as it will be further discussed by DFT studies in the 3.5 section.

The mass spectrum of the gold(I) complex shows a peak corresponding to the $[Au(C_{18}H_{15}P)(C_{18}H_{13}N_4O_5S) + H]^+$ ion at *m/z* 857.08. Ligand scrambling reactions of the gold(I) complex can be observed with the formation of the $[Au_2(C_{18}H_{15}P)_2(C_{18}H_{12}N_4O_5S) + H]^+$ ion at *m/z* 1315.18, where two (phosphine)gold units are present. This is a common feature found in the literature [44,45]. This species probably does not exist in solid form, as confirmed by other techniques. The gold isotopic pattern of the two species can be observed in **Figure 5**. The peak at *m/z* 399.05 corresponds to the free ionized sulfasalazine $[(C_{18}H_{14}N_4O_5S) + H]^+$ and the peak at *m/z* 102.11 corresponds to the ionized triethylamine. This result confirms the proposed composition for this complex as suggested by elemental and thermal analyses, and the presence of one triethylamine molecule in the complex.

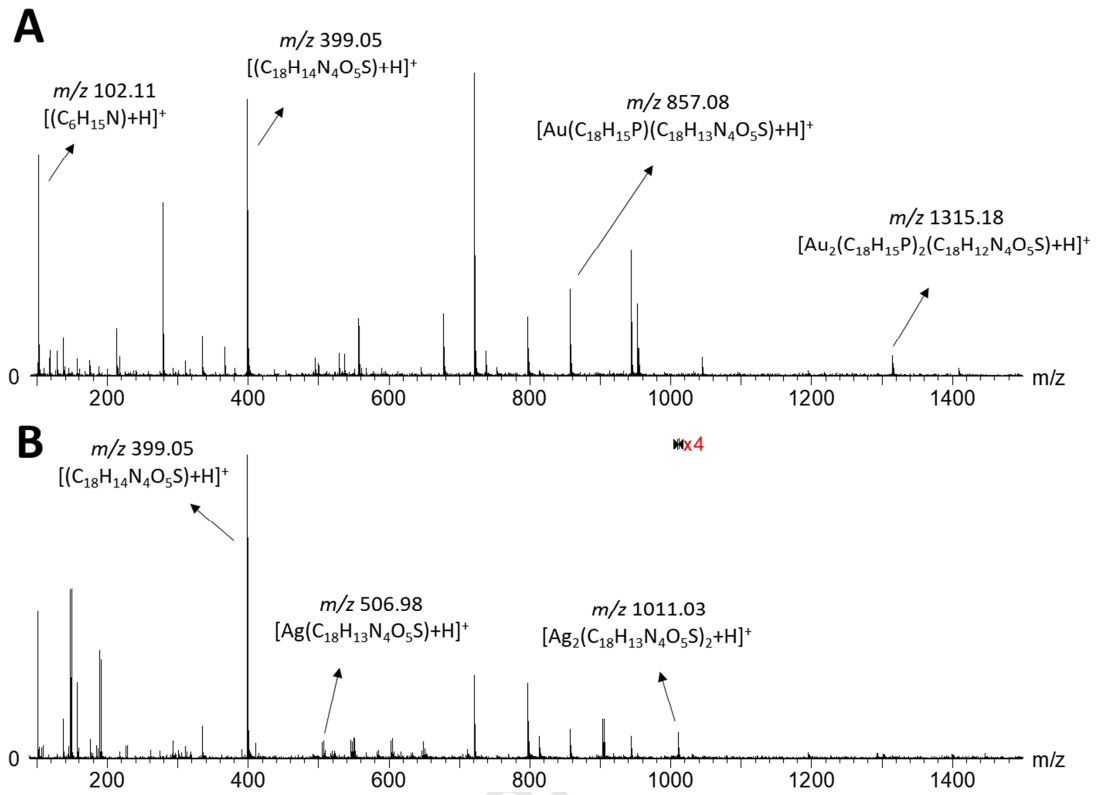

Fig. 3. ESI(+)-QTOF mass spectrum for (A) gold and (B) silver complex from *m/z* 90 to 1500.

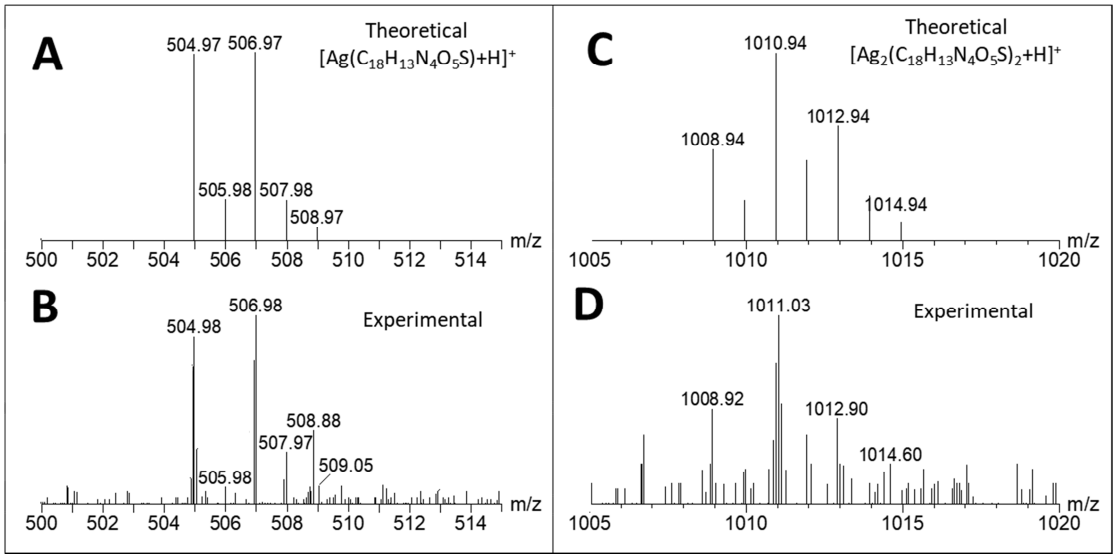

Fig. 4. Theoretical isotopic distribution of (A) $[Ag(C_{18}H_{13}N_4O_5S) + H]^+$ and (C) $[Ag_2(C_{18}H_{13}N_4O_5S)_2 + H]^+$ in comparison with their respective experimental data at (B) *m/z* 506.98, (D) *m/z* 1011.03.

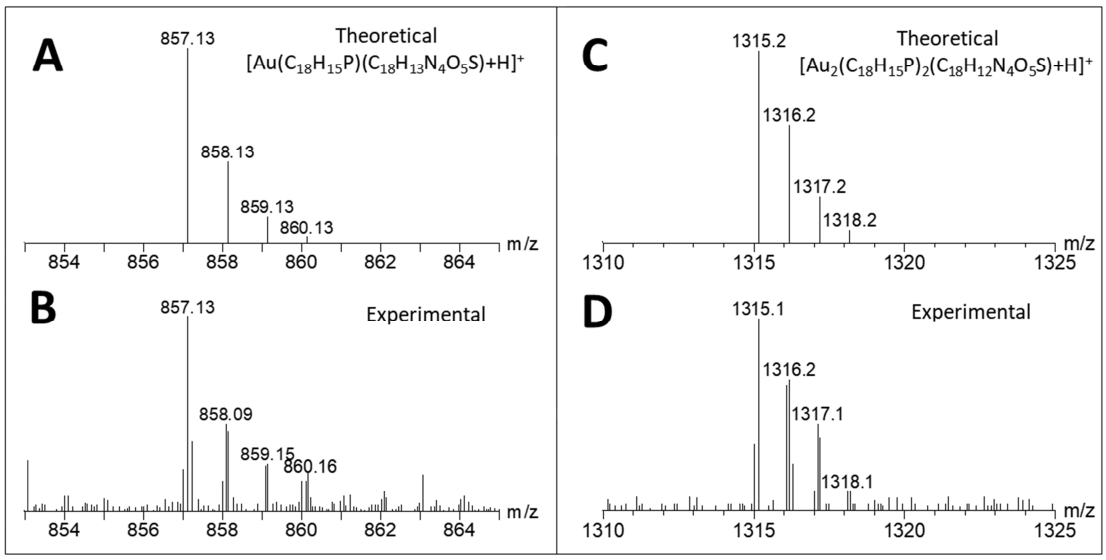

Fig. 5. Theoretical isotopic distribution of (A) $[Au(C_{18}H_{15}P)(C_{18}H_{13}N_4O_5S) + H]^+$ and (C) $[Au_2(C_{18}H_{15}P)_2(C_{18}H_{12}N_4O_5S) + H]^+$ in comparison with their respective experimental data at (B) *m/z* 857.13 and (D) *m/z* 1315.2.

3.5. DFT studies

The infrared, NMR and mass spectrometric data provided essential information regarding the composition and coordination sphere for the silver(I) and gold(I) complexes. This information was used to draw the starting geometries that were subject to DFT optimization. The final optimized structures can be found in **Figure 6.** In the case of the silver complex the combination of the theoretical (DFT) and experimental data led us to propose a dimeric structure for the compound, where each sulfasalazine bridges between two silver atoms by the carboxylate group. For the gold(I) complex a monomeric structure has shown to be the most stable one. The bond lengths and angles obtained for the optimized structures are shown in **Table 2.** Atomic coordinates for the gold(I) complex are presented in the **Supplementary Material File A**, while for the silver(I) complex the atomic coordinates can be found in the **Supplementary Material File B.**

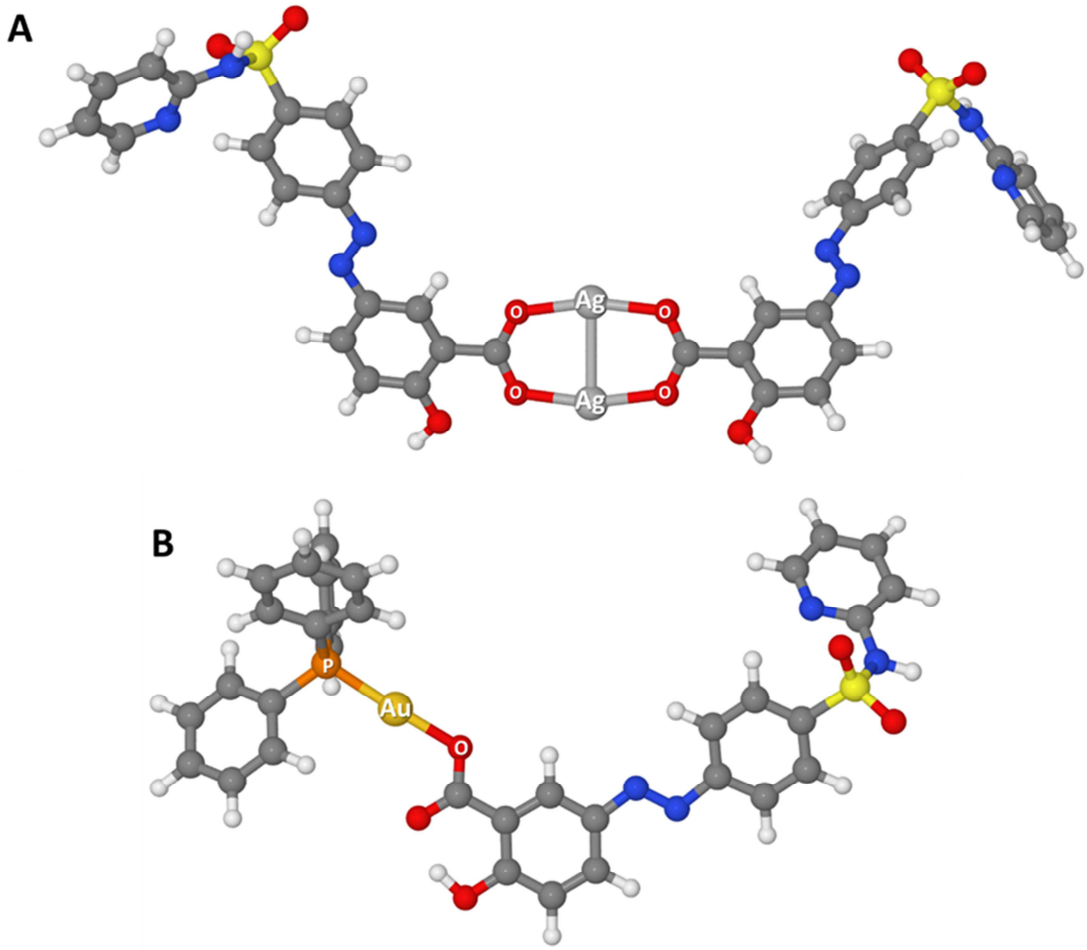

Fig. 6. DFT-optimized structures of (A) silver(I) and (B) gold(I) complexes. The atoms that are part of the coordination spheres are labeled, as well as the metal ions. The remaining atoms follow the typical color code: Nitrogen - blue; Carbon – dark grey; sulfur - yellow.

Table 2. Selected bond lengths and angles for the DFT-optimized structures of silver(I) and gold(I) complexes studied in this work.

silver complex			
Atoms	Bond length (Å)	Atoms	Angle (°)
Ag-O	2.113	O-Ag-O	165.3
	2.110		165.0
	2.117	O-C-O	127.2
	2.119		126.8
Ag-Ag	2.802		
C-O	1.262		
	1.256		
	1.262		
	1.258		

N=N	1.247		
	1.248		
Gold(I) complex			
Atoms	Bond length (Å)	Atoms	Angle (°)
Au-P	2.226	P-Au-O	176.4
Au-O	2.041		
N=N	1.247		

The cage-like arrangement observed for the silver(I) complex, which corresponds to the $[Ag(ssz)]_2$ coordination formula, is typical for silver complexes with carboxylate-containing ligands and it is in good agreement with the experimental data for the silver complex with sulfasalazine. One of the best examples of this kind of arrangement is the silver-acetate complex, where the structure contains $[Ag_2(carboxylate)_2]$ dimer units [46]. This kind of carboxylate coordination can also be seen in the crystal structure of a metal-organic framework containing silver and 4,4'-bipyridine and salicylate as ligands. The salicylate acts as a bidentate bridging ligand between two silver atoms in a similar way of that suggested in our case [47]. Another example is the silver(I) complex with the anti-inflammatory drug ibuprofen, $[Ag(ibu)]_2$, where each molecule of the ligand bridges between two silver atoms by the carboxylate group in a very similar fashion of the silver(I) complex described here [48].

The double carboxylate-supported dimeric silver complexes comprise one of the classes of silver compounds that present argentophilic interactions [49]. The crystal structure of a representative example of this class of compounds, the silver(I) 3,5-dimethylbenzoate, has an Ag-Ag interaction of 2.7719 Å [50]. This short interaction agrees with the Ag-Ag distance found by DFT for the $[Ag(ssz)]_2$ complex, where the argentophilic interaction is of 2.802 Å as observed in **Table 2**.

A monodentate coordination of carboxylate to the (phosphine)gold(I) motif is also a common structural feature. It can be observed, for example, in the crystal structure of $[(Ph_3P)Au(acetate)]$ [51], and in the structure of many (phosphine)gold compounds with fluorocarboxylates [52]. In the review article of Grodzicki et al., a series of (phosphine)gold(I) complexes are described and, in all cases, coordination by a monodentate mode is observed [53]. Such evidences reinforce the suggested coordination formula for the gold(I) complex as $[(Ph_3P)Au(ssz)]$.

3.6. Minimum inhibitory concentration (MIC)

Antibacterial activity assays were performed to evaluate the antibacterial activity of the $[Ag(ssz)]_2$ and $[(Ph_3P)Au(ssz)]$ complexes and to compare it with the activities of the free ligand against Gram-positive (*S. aureus* and *B. cereus*) and Gram-negative (*E. coli* and *P. aeruginosa*) strains. The experimental results are summarized in **Table 3**. As a positive control, silver nitrate was used, which presented a MIC value < 31.25 $\mu g \cdot mL^{-1}$ for all strains tested.

The free ligand did not exhibit antibacterial activity *in vitro* for any of the tested bacterial strains in the considered experimental conditions. On the other hand, with coordination of ssz to silver and gold metal ions, it was possible to observe inhibition of the bacterial strains, as evidenced by the MIC values. The $[Ag(ssz)]_2$ complex showed better activity against *S. aureus*, with a MIC value of 500 $\mu g \cdot mL^{-1}$ (0.495 mmol L^{-1}). For the $[(Ph_3P)Au(ssz)]$ complex, the lowest MIC found was of 62.5 $\mu g \cdot mL^{-1}$ (0.065 mmol L^{-1}) against *B. cereus*, which was even more active than the gold(I) precursor $[(Ph_3P)AuCl]$. This particular result clearly demonstrates the contribution of sulfasalazine and the gold(phosphine) moiety to the antibacterial activity of the $[(Ph_3P)Au(ssz)]$ complex.

Comparing the results here presented with other silver(I) complexes with sulfonamides described in the literature, it was possible to evaluate that the $[Ag(ssz)]_2$ complex has similar MIC values and, in some cases, they have shown to be active in lower concentrations than those already described. The sulfamethizole [33], sulfamethoxazole and sulfathiazole [30] complexes with silver(I) presented MIC values of 3.31, 13.9 and 6.90 mmol L^{-1}, respectively, against *S. aureus*, and 0.41, 1.74 and 3.45 against *P. aeruginosa*. Silver sulfadiazine, which is clinically used, shows MIC values from 0.045 to 0.360 mmol L^{-1} for *S. aureus*, a result that can be compared with that obtained for the $[Ag(ssz)]_2$ and $[(Ph_3P)Au(ssz)]$ complexes [54]. The solubility of the complexes with sulfasalazine in DMSO may also be considered as an advantage over AgSSD and warrants for further studies considering a possible application for the treatment of skin infections.

Table 3. Minimum inhibitory concentration (MIC) values.

Compounds	MIC μg mL^{-1} (mmol L^{-1})			
	S. aureus	***B. cereus***	***E. coli***	***P. aeruginosa***
Ssz	R	R	R	R
$[Ag(ssz)]_2$	500 (0.495)	1000 (0.990)	2000 (1.979)	1000 (0.990)
$[(Ph_3P)Au(ssz)]$	2000 (2.088)	62.5 (0.065)	1000 (1.044)	500 (0.522)
$[(Ph_3P)AuCl]$	500 (1.011)	125 (0.253)	250 (0.505)	125 (0.253)
$AgNO_3$	< 31.25 (< 0.184)	< 31.25 (< 0.184)	< 31.25 (< 0.184)	< 31.25 (< 0.184)

R = resistant.

Although silver nitrate exhibits MIC values lower than those observed for the silver(I) and gold(I) complexes, it is already well-known in the literature that this salt is toxic to health tissues in concentrations higher than 1%. Moreover, the light instability and the fast and uncontrolled release of silver ions from silver nitrate have limited its application in the clinics [31,55,56]. Nevertheless, further cytotoxic activity assays of the complexes are necessary to compare with the cytotoxicity of silver nitrate and to determine the safety of the complexes described here.

3.7. Interaction studies of the complexes with pGEX-4T1 DNA plasmid by agarose gel electrophoresis

Considering the antibacterial activities exhibited by the new $[Ag(ssz)]_2$ and $[(Ph_3P)Au(ssz)]$ complexes, agarose gel electrophoresis assays were performed to investigate if DNA is one of the possible targets for the compounds. In this case, pGEX-4T1 plasmid DNA was used. For comparative purposes, K_2PdCl_4 and cisplatin ($[PtCl_2(NH_3)_2]$), which are known for interacting with DNA, were used as positive controls (**Figure 7**) [57–60].

The experimental results show modifications in the electrophoretic profile of the plasmid with cisplatin at both concentrations, more specifically in the first band, which is attributed to the open circular (OC) form of the plasmid, and in the middle bands that are attributed to the linear form (LF) [61]. The interaction of K_2PdCl_4 with the pGEX-4T1 plasmid is the most pronounced one, where we can see that all bands were affected by the palladium(II) salt evidencing a strong interaction with DNA, as expected. However, evidences of interaction of the ligand or the silver(I) and gold(I) complexes with the plasmid were not detected. These results show that these compounds do not

interact with DNA as cisplatin or K_2PdCl_4. Silver nitrate and the gold precursor [$(Ph_3P)AuCl$] also did not show evidences of interaction with DNA. Further studies with other biomolecules, such as proteins may also be envisaged to ascertain the possible molecular target of the complexes with sulfasalazine.

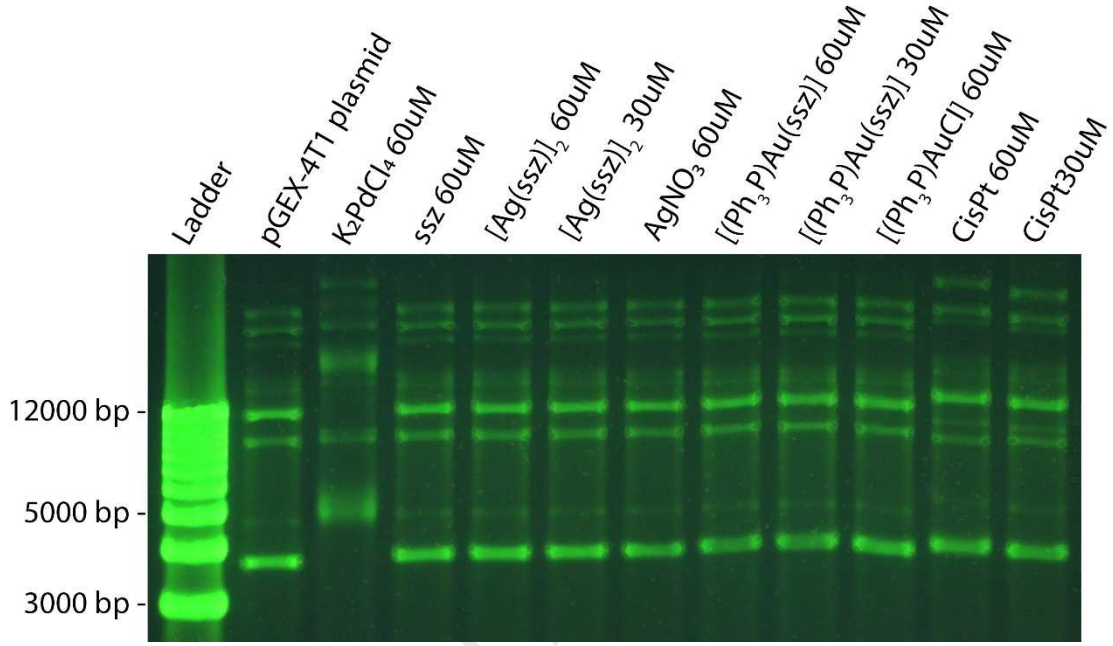

Fig. 7. Results of the agarose gel electrophoresis of the pGEX-4T1 plasmid DNA in the presence of K_2PdCl_4, ssz, $[Ag(ssz)]_2$, $AgNO_3$, [$(Ph_3P)Au(ssz)$], [$(Ph_3P)AuCl$] and cisplatin (CisPt).

Conclusion

New complexes of silver(I) and gold(I) with sulfasalazine, with minimal formulas $AgC_{18}H_{13}N_4O_5S$ and $AuPC_{36}H_{28}N_4O_5S{\cdot}N(CH\square CH\square)\square$, were obtained. Infrared and ^{1}H and ^{13}C NMR studies permitted proposing that sulfasalazine coordinates to silver(I) by the carboxylate group in a bidentate bridging mode, while for the gold(I) complex coordination of the carboxylate occurs in a monodentate form. The presence of the $[Ag(C_{18}H_{13}N_4O_5S) + H]^+$ and $[Ag_2(C_{18}H_{13}N_4O_5S)_2 + H]^+$ monoprotonated species in the mass spectra suggests that the silver(I) complex exists in a dimeric form. For the gold(I) complex, the $[Au(C_{18}H_{15}P)(C_{18}H_{13}N_4O_5S) + H]^+$ ion was identified. DFT studies combined with the experimental analyses led us to propose the coordination formulas of the silver(I) and gold(I) species, where a dimeric structure for the silver(I) complex and a monomeric one for the gold(I) complex have shown to be the most stable ones.

Antibacterial studies showed that both complexes are active against Gram-positive (*S. aureus* and *B. cereus*) and Gram-negative (*E. coli* and *P. aeruginosa*) strains. The gold(I) complex has shown to be more active over *B. cereus*, with MIC value of 62.5 µg mL^{-1} (0.065 mmol L^{-1}), while the silver(I) complex has shown to be more active over *S. aureus* bacterial strain, with MIC value of 500 µg mL^{-1} (0.495 mmol L^{-1}). The antibacterial activities observed for the $[Ag(ssz)]_2$ and $[(Ph_3P)Au(ssz)]$ complexes in comparison to the free ligand demonstrate that the coordination of metal ions to bioactive ligands is an interesting strategy that can be further explored. The observed results are closely related to those found for AgSSD, which is clinically used for treatment of skin infections. Gel electrophoresis assays with pGEX-4T1 plasmid DNA were performed, but no interactions of both complexes with DNA were observed. Such results led us to conclude that DNA is not a preferential biomolecular target for the complexes.

Disclosure statement

No potential conflict of interest was reported by the authors.

Acknowledgments

This study was supported by grants from the Brazilian Agencies FAPESP (São Paulo State Research Council, Grants # 2015/09833-0, 2017/25995-6, 2018/12590-0 and 2018/12062-4) and CNPq (National Council of Scientific and Technological Development, Grant # 407012/2018-4). Also, this study was financed in part by the Coordenação de Aperfeiçoamento de Pessoal de Nível Superior - Brasil (CAPES) - Finance Code 001. Dr. de Paiva also would like to thank the research developed with high performance computation resources provided by the IT Superintendence of the University of São Paulo, USP, Brazil.

References

[1] Antibiotic resistance, World Health Organ. - WHO. (2018). https://www.who.int/news-room/fact-sheets/detail/antibiotic-resistance (accessed November 2, 2019).

[2] About Antimicrobial Resistance, Cent. Dis. Control Prev. CDC. (2018). https://www.cdc.gov/drugresistance/about.html (accessed November 2, 2019).

[3] C.L. Ventola, The antibiotic resistance crisis: part 1: causes and threats, P T Peer-Rev. J. Formul. Manag. 40 (2015) 277–283.
[4] S. Medici, M. Peana, V.M. Nurchi, J.I. Lachowicz, G. Crisponi, M.A. Zoroddu, Noble metals in medicine: Latest advances, Coord. Chem. Rev. 284 (2015) 329–350. https://doi.org/10.1016/j.ccr.2014.08.002.
[5] A.F. Santos, D.F. Brotto, L.R.V. Favarin, N.A. Cabeza, G.R. Andrade, M. Batistote, A.A. Cavalheiro, A. Neves, D.C.M. Rodrigues, A. dos Anjos, Study of the antimicrobial activity of metal complexes and their ligands through bioassays applied to plant extracts, Rev. Bras. Farmacogn. 24 (2014) 309–315. https://doi.org/10.1016/j.bjp.2014.07.008.
[6] D.P. Rocha, G.F. Pinto, R. Ruggiero, C.A. de Oliveira, W. Guerra, A.P.S. Fontes, T.T. Tavares, I.M. Marzano, E.C. Pereira-Maia, Coordenação de metais a antibióticos como uma estratégia de combate à resistência bacteriana, Quím. Nova. 34 (2011) 111–118. https://doi.org/10.1590/S0100-40422011000100022.
[7] M. Rizzotto, Chapter: 15. Metal Complexes as Antimicrobial Agents, in: Seach Antibact. Agents, INTECH Open Access Publisher, Croatia, 2012: pp. 73–88.
[8] F.A. Saad, H.A. El-Ghamry, M.A. Kassem, A.M. Khedr, Nano-synthesis, Biological Efficiency and DNA Binding Affinity of New Homo-binuclear Metal Complexes with Sulfa Azo Dye Based Ligand for Further Pharmaceutical Applications, J. Inorg. Organomet. Polym. Mater. 29 (2019) 1337–1348. https://doi.org/10.1007/s10904-019-01098-z.
[9] M. Pervaiz, A. Riaz, A. Munir, Z. Saeed, S. Hussain, A. Rashid, U. Younas, A. Adnan, Synthesis and characterization of sulfonamide metal complexes as antimicrobial agents, J. Mol. Struct. 1202 (2020) 127284. https://doi.org/10.1016/j.molstruc.2019.127284.
[10] Z.H. Chohan, Metal-based sulfonamides: Their preparation, characterization and *in-vitro* antibacterial, antifungal & cytotoxic properties. X-ray structure of 4-[(2-hydroxybenzylidene) amino] benzenesulfonamide, J. Enzyme Inhib. Med. Chem. 23 (2008) 120–130. https://doi.org/10.1080/14756360701384195.
[11] Z.H. Chohan, H.A. Shad, M.H. Youssoufi, T. Ben Hadda, Some new biologically active metal-based sulfonamide, Eur. J. Med. Chem. 45 (2010) 2893–2901. https://doi.org/10.1016/j.ejmech.2010.03.014.
[12] O. Sköld, Sulfonamide resistance: mechanisms and trends, Drug Resist. Updat. 3 (2000) 155–160. https://doi.org/10.1054/drup.2000.0146.
[13] P. Silva, Farmacologia, Guanabara Koogan, Rio de Janeiro, 2006.
[14] M.G.N. El-Wahed, M.S. Refat, S.M. El-Megharbel, Spectroscopic, thermal and biological studies of coordination compounds of sulfasalazine drug: Mn(II), Hg(II), Cr(III), ZrO(II), VO(II) and Y(III) transition metal complexes, Bull. Mater. Sci. 32 (2009) 205–214. https://doi.org/10.1007/s12034-009-0032-x.
[15] C. Astbury, A.J. Taggart, L. Juby, L. Zebouni, H.A. Bird, Comparison of the single dose pharmacokinetics of sulphasalazine in rheumatoid arthritis and inflammatory bowel disease, Ann. Rheum. Dis. 49 (1990) 587–590. https://doi.org/10.1136/ard.49.8.587.
[16] R. Bentley, Different roads to discovery; Prontosil (hence sulfa drugs) and penicillin (hence β-lactams), J. Ind. Microbiol. Biotechnol. 36 (2009) 775–786. https://doi.org/10.1007/s10295-009-0553-8.
[17] R.B. Stein, G.R. Lichtenstein, Medical therapy for Crohn's disease: the state of the art, Surg. Clin. North Am. 81 (2001) 71–101. https://doi.org/10.1016/S0039-6109(05)70274-7.

[18] Z.-F. Chen, S. Kang, H. Liang, F. Yi, K.-B. Yu, R.-G. Xiong, X.-Z. You, Crystallographic report: Crystal structure of the first alkaline earth metal compound with the antibacterial drug sulfasalazine: $[Sr(H\text{-}Sulf)(H_2O)_6](H\text{-}Sulf)\cdot 3H_2O$: Main Group Metal Compounds, Appl. Organomet. Chem. 17 (2003) 887–888. https://doi.org/10.1002/aoc.539.

[19] M.V. Ol'khovich, A.V. Sharapova, S.V. Blokhina, G.L. Perlovich, Sulfasalazine: Dissolution and Distribution in Pharmaceutically Relevant Mediums, J. Chem. Eng. Data. 62 (2017) 123–128. https://doi.org/10.1021/acs.jced.6b00497.

[20] F.A. Saad, Elaborated molecular docking and DFT/B3LYP studies for novel sulfa drug complexes, spectral and antitumor investigations, J. Therm. Anal. Calorim. 129 (2017) 425–440. https://doi.org/10.1007/s10973-016-6017-2.

[21] A. Casini, A. Scozzafava, A. Mastrolorenzo, C. Supuran, Sulfonamides and Sulfonylated Derivatives as Anticancer Agents, Curr. Cancer Drug Targets. 2 (2002) 55–75. https://doi.org/10.2174/1568009023334060.

[22] C.N. Banti, C. Papatriantafyllopoulou, M. Manoli, A.J. Tasiopoulos, S.K. Hadjikakou, Nimesulide Silver Metallodrugs, Containing the Mitochondriotropic, Triaryl Derivatives of Pnictogen; Anticancer Activity against Human Breast Cancer Cells, Inorg. Chem. 55 (2016) 8681–8696. https://doi.org/10.1021/acs.inorgchem.6b01241.

[23] M. Nagane, E. Kanai, Y. Shibata, T. Shimizu, C. Yoshioka, T. Maruo, T. Yamashita, Sulfasalazine, an inhibitor of the cystine-glutamate antiporter, reduces DNA damage repair and enhances radiosensitivity in murine B16F10 melanoma, PLOS ONE. 13 (2018) e0195151. https://doi.org/10.1371/journal.pone.0195151.

[24] M.S. Refat, S.F. Mohamed, Spectroscopic, thermal and antitumor investigations of sulfasalazine drug, *in situ* complexation with alkaline earth metal ions, Spectrochim. Acta. A. Mol. Biomol. Spectrosc. 82 (2011) 108–117. https://doi.org/10.1016/j.saa.2011.07.010.

[25] K.-B. Huang, Y.-S. Tan, X.-Y. Song, Y.-C. Liu, Z.-F. Chen, (Sulfasalazinato-κ *O*)bis(triphenylphosphine-κ *P*)copper(I), Acta Crystallogr. Sect. E Struct. Rep. Online. 66 (2010) m549–m550. https://doi.org/10.1107/S1600536810013899.

[26] C.R. Mizdal, S.T. Stefanello, V. da C. Flores, V.A. Agertt, P.C. Bonez, G.G. Rossi, T.C. da Silva, F.A. A. Soares, L. de L. Marques, M.M.A. de Campos, The antibacterial and anti-biofilm activity of gold-complexed sulfonamides against methicillin-resistant Staphylococcus aureus, Microb. Pathog. 123 (2018) 440–448. https://doi.org/10.1016/j.micpath.2018.08.002.

[27] C. Aguzzi, G. Sandri, C. Bonferoni, P. Cerezo, S. Rossi, F. Ferrari, C. Caramella, C. Viseras, Solid state characterisation of silver sulfadiazine loaded on montmorillonite/chitosan nanocomposite for wound healing, Colloids Surf. B Biointerfaces. 113 (2014) 152–157. https://doi.org/10.1016/j.colsurfb.2013.08.043.

[28] F. Velluti, N. Mosconi, A. Acevedo, G. Borthagaray, J. Castiglioni, R. Faccio, D.F. Back, G. Moyna, M. Rizzotto, M.H. Torre, Synthesis, characterization, microbiological evaluation, genotoxicity and synergism tests of new nano silver complexes with sulfamoxole: X-ray diffraction of $[Ag_2(SMX)_2]\cdot$DMSO, J. Inorg. Biochem. 141 (2014) 58–69. https://doi.org/10.1016/j.jinorgbio.2014.08.007.

[29] R.E.F. de Paiva, C. Abbehausen, A.F. Gomes, F.C. Gozzo, W.R. Lustri, A.L.B. Formiga, P.P. Corbi, Synthesis, spectroscopic characterization, DFT studies and antibacterial assays of a novel silver(I) complex with the anti-inflammatory nimesulide, Polyhedron. 36 (2012) 112–119. https://doi.org/10.1016/j.poly.2012.02.002.

[30] J.H. Bormio Nunes, R.E.F. de Paiva, A. Cuin, W.R. Lustri, P.P. Corbi, Silver complexes with sulfathiazole and sulfamethoxazole: Synthesis, spectroscopic characterization, crystal structure and antibacterial assays, Polyhedron. 85 (2015) 437–444. https://doi.org/10.1016/j.poly.2014.09.010.

[31] A.T.M. Fiori, D.H. Nakahata, A. Cuin, W.R. Lustri, P.P. Corbi, Synthesis, crystallographic studies, high resolution mass spectrometric analyses and antibacterial assays of silver(I) complexes with sulfisoxazole and sulfadimethoxine, Polyhedron. 121 (2017) 172–179. https://doi.org/10.1016/j.poly.2016.09.046.

[32] D.H. Nakahata, W.R. Lustri, A. Cuin, P.P. Corbi, Crystal structure, spectroscopic characterization and antibacterial activities of a silver complex with sulfameter, J. Mol. Struct. 1125 (2016) 609–615. https://doi.org/10.1016/j.molstruc.2016.07.049.

[33] L.M. Yamamoto, J.H.B. Nunes, M.A. Ribeiro, A.M. da C. Ferreira, W.R. Lustri, P.P. Corbi, Copper(II) and silver(I) complexes with sulfamethizole: synthesis, spectroscopic characterization, ESI-QTOF mass spectrometric analysis, crystal structure and antibacterial activities, Polyhedron. 138 (2017) 168–176. https://doi.org/10.1016/j.poly.2017.09.034.

[34] D.H. Nakahata, R.E.F. de Paiva, W.R. Lustri, C.M. Ribeiro, F.R. Pavan, G.G. da Silva, A.L.T.G. Ruiz, J.E. de Carvalho, P.P. Corbi, Sulfonamide-containing copper(II) metallonucleases: Correlations with in vitro antimycobacterial and antiproliferative activities, J. Inorg. Biochem. 187 (2018) 85–96. https://doi.org/10.1016/j.jinorgbio.2018.07.011.

[35] F. Neese, Software update: the ORCA program system, version 4.0, Wiley Interdiscip. Rev. Comput. Mol. Sci. 8 (2018) 1–6. https://doi.org/10.1002/wcms.1327.

[36] F. Neese, The ORCA program system, Wiley Interdiscip. Rev. Comput. Mol. Sci. 2 (2012) 73–78. https://doi.org/10.1002/wcms.81.

[37] F. Weigend, Accurate Coulomb-fitting basis sets for H to Rn, Phys. Chem. Chem. Phys. 8 (2006) 1057–1065. https://doi.org/10.1039/b515623h.

[38] Clinical and Laboratory Standards Institute (CLSI), Performance Standards for Antimicrobial Susceptibility Testing, Twenty-six ed., Committee for Clinical Laboratory Standards, Wayne, 2016.

[39] S.Q. Gomes, L. Vitoriano, E.G.R. de Arruda, A.L.T.G. Ruiz, T. Candido, J.E. de Carvalho, W.R. Lustri, C. Abbehausen, Linear gold(I) complex with tris-(2-carboxyethyl)phosphine (TCEP): Selective antitumor activity and inertness toward sulfur proteins, J. Inorg. Biochem. 186 (2018) 104–115. https://doi.org/10.1016/j.jinorgbio.2018.04.005.

[40] M.R. Ciol, C.M. Manzano, A. Cuin, F.R. Pavan, C.M. Ribeiro, A.L.T.G. Ruiz, E.C.S. de Oliveira, W.R. Lustri, N.F. Fregonezi, F.A.R. Nogueira, P.P. Corbi, A Silver Complex with Cycloserine: Synthesis, Spectroscopic Characterization, Crystal Structure and *In Vitro* Biological Studies, ChemistrySelect. 3 (2018) 1719–1726. https://doi.org/10.1002/slct.201703078.

[41] A.T. Fiori-Duarte, F.R.G. Bergamini, R.E.F. de Paiva, C.M. Manzano, W.R. Lustri, P.P. Corbi, A new palladium(II) complex with ibuprofen: Spectroscopic characterization, DFT studies, antibacterial activities and interaction with biomolecules, J. Mol. Struct. 1186 (2019) 144–154. https://doi.org/10.1016/j.molstruc.2019.03.020.

[42] K. Nakamoto, Infrared and Raman Spectra of Inorganic and Coordination Compounds Part B: Applications in Coordination, Organometallic, and Bioinorganic Chemistry, sixth ed., John Wiley & Sons, New York, 2009.

[43] M.S. Refat, S.A. El-Korashy, I.M. El-Deen, S.M. El-Sayed, Experimental and spectroscopic studies of charge transfer reaction between sulfasalazine antibiotic drug with different types of acceptors, Drug Test. Anal. 3 (2011) 116–131. https://doi.org/10.1002/dta.178.

[44] S.G.T. Kazimi, M.S. Iqbal, C.C. Mulligan, C. Frank Shaw, F. Iram, A.R. Stelmack, I.S. Campbell, Ligand Exchange/Scrambling Study of Gold(I)-Phosphine Complexes in the Solid Phase by DESI-MS Analysis, J. Am. Soc. Mass Spectrom. 30 (2019) 2289–2296. https://doi.org/10.1007/s13361-019-02319-y.

[45] A.L. Hormann-Arendt, C.F. Shaw, Ligand-scrambling reactions of cyano(trialkyl/triarylphosphine)gold(I) complexes: examination of factors influencing the equilibrium constant, Inorg. Chem. 29 (1990) 4683–4687. https://doi.org/10.1021/ic00348a019.

[46] L.P. Olson, D.R. Whitcomb, M. Rajeswaran, T.N. Blanton, B.J. Stwertka, The Simple Yet Elusive Crystal Structure of Silver Acetate and the Role of the Ag−Ag Bond in the Formation of Silver Nanoparticles during the Thermally Induced Reduction of Silver Carboxylates, Chem. Mater. 18 (2006) 1667–1674. https://doi.org/10.1021/cm052657v.

[47] H. Wu, Z. Yang, F. Wang, H. Zhang, H. Peng, C. Wang, Crystal structure, DNA-binding properties and antioxidative activities of a novel silver(I) inorganic polymer, Res. Chem. Intermed. 42 (2016) 2473–2485. https://doi.org/10.1007/s11164-015-2162-7.

[48] I.M.P. e Silva, D. de M. Profirio, R.E.F. de Paiva, M. Lancellotti, A.L.B. Formiga, P.P. Corbi, A silver complex with ibuprofen: Synthesis, solid state characterization, DFT calculations and antibacterial assays, J. Mol. Struct. 1049 (2013) 1–6. https://doi.org/10.1016/j.molstruc.2013.06.034.

[49] H. Schmidbaur, A. Schier, Argentophilic Interactions, Angew. Chem. Int. Ed. 54 (2015) 746–784. https://doi.org/10.1002/anie.201405936.

[50] Y. Wang, U. Englert, Homo- and heterochiral coordination polymers of silver with diaminocyclohexane as bridging ligand: Trends in alkylbenzoates, Inorganica Chim. Acta. 363 (2010) 2539–2545. https://doi.org/10.1016/j.ica.2010.04.030.

[51] P.G. Jones, Acetato(triphenylphosphine)gold(I), [Au($C_2H_3O_2$)($C_{18}H_{15}P$)], Acta Crystallogr. C. 40 (1984) 1320–1322. https://doi.org/10.1107/S0108270184007812.

[52] P. Römbke, A. Schier, H. Schmidbaur, Gold(I) Carboxylates and Fluorocarboxylates, Z. Für Naturforschung B. 57 (2002) 605–609. https://doi.org/10.1515/znb-2002-0602.

[53] A. Grodzicki, I. Łakomska, P. Piszczek, I. Szymańska, E. Szłyk, Copper(I), silver(I) and gold(I) carboxylate complexes as precursors in chemical vapour deposition of thin metallic films, Coord. Chem. Rev. 249 (2005) 2232–2258. https://doi.org/10.1016/j.ccr.2005.05.026.

[54] J.M.T. Hamilton-Miller, S. Shah, C. Smith, Silver Sulphadiazine: A Comprehensive in vitro Reassessment, Chemotherapy. 39 (1993) 405–409. https://doi.org/10.1159/000238985.

[55] C.L. Fox, S.M. Modak, Mechanism of Silver Sulfadiazine Action on Burn Wound Infections, Antimicrob. Agents Chemother. 5 (1974) 582–588. https://doi.org/10.1128/AAC.5.6.582.

[56] B.S. Atiyeh, M. Costagliola, S.N. Hayek, S.A. Dibo, Effect of silver on burn wound infection control and healing: Review of the literature, Burns. 33 (2007) 139–148. https://doi.org/10.1016/j.burns.2006.06.010.

[57] N.Yu. Fomina, O.A. Chaplygina, A.D. Shebaldova, V.B. Borodulin, Reaction of K_2PdCl_4 with synthetic and natural nucleic acids, Russ. J. Gen. Chem. 72 (2002) 704–709. https://doi.org/10.1023/A:1019595815958.
[58] H.C. Harder, B. Rosenberg, Inhibitory effects of anti-tumor platinum compounds on DNA, RNA and protein syntheses in mammalian cells *in vitro*, Int. J. Cancer. 6 (1970) 207–216. https://doi.org/10.1002/ijc.2910060207.
[59] P.M. Takahara, A.C. Rosenzweig, C.A. Frederick, S.J. Lippard, Crystal structure of double-stranded DNA containing the major adduct of the anticancer drug cisplatin, Nature. 377 (1995) 649–652. https://doi.org/10.1038/377649a0.
[60] A.C. Komor, J.K. Barton, The path for metal complexes to a DNA target, Chem. Commun. 49 (2013) 3617–3630. https://doi.org/10.1039/c3cc00177f.
[61] J. Cebrián, M.J. Kadomatsu-Hermosa, A. Castán, V. Martínez, C. Parra, M.J. Fernández-Nestosa, C. Schaerer, M.-L. Martínez-Robles, P. Hernández, D.B. Krimer, A. Stasiak, J.B. Schvartzman, Electrophoretic mobility of supercoiled, catenated and knotted DNA molecules, Nucleic Acids Res. 43 (2015) 1–10. https://doi.org/10.1093/nar/gku1255.

Fig. Captions

Fig. 1. Structure of sulfasalazine with carbon, hydrogen and nitrogen atoms numbered.

Fig. 2. ^{1}H NMR spectra in DMSO-d_6 of (A) sulfasalazine, (B) silver(I) complex and (C) gold(I). The extrapolated spectra are given in detail to show the signals corresponding to H7, H20 and H22.

Fig. 3. ESI(+)-QTOF mass spectrum for (A) gold and (B) silver complex from *m/z* 90 to 1500.

Fig. 4. Theoretical isotopic distribution of (A) $[Ag(C_{18}H_{13}N_4O_5S) + H]^+$ and (C) $[Ag_2(C_{18}H_{13}N_4O_5S)_2 + H]^+$ in comparison with their respective experimental data at (B) *m/z* 506.98, (D) *m/z* 1011.03.

Fig. 5. Theoretical isotopic distribution of (A) $[Au(C_{18}H_{15}P)(C_{18}H_{13}N_4O_5S) + H]^+$ and (C) $[Au_2(C_{18}H_{15}P)_2(C_{18}H_{12}N_4O_5S) + H]^+$ in comparison with their respective experimental data at (B) *m/z* 857.13 and (D) *m/z* 1315.2.

Fig. 6. DFT-optimized structures of (A) silver(I) and (B) gold(I) complexes. The atoms that are part of the coordination spheres are labeled, as well as the metal ions. The

remaining atoms follow the typical color code: Nitrogen - blue; Carbon – dark grey; sulfur - yellow.

Fig. 7. Results of the agarose gel electrophoresis of the pGEX-4T1 plasmid DNA in the presence of K_2PdCl_4, ssz, $[Ag(ssz)]_2$, $AgNO_3$, $[(Ph_3P)Au(ssz)]$, $[(Ph_3P)AuCl]$ and cisplatin (CisPt).

Highlights

► Novel silver and gold complexes with the sulfonamide drug sulfasalazine are presented. ► Spectroscopic studies indicate ligand coordination to metal ions by carboxylate group. ► Theoretical and experimental data permitted proposing the structures of the complexes. ► The complexes are active over Gram-positive and Gram-negative bacterial strains. ► Agarose gel electrophoresis showed the non-interaction of the complexes with DNA.

Declaration of interests

☒ The authors declare that they have no known competing financial interests or personal relationships that could have appeared to influence the work reported in this paper.

☐The authors declare the following financial interests/personal relationships which may be considered as potential competing interests: